IMAGING UPPER-CRUSTAL CONVECTION PLUMES BENEATH THE TAUPO VOLCANIC ZONE, NEW ZEALAND

Bertrand E.A.[1], Caldwell T.G.[1], Bannister S.B.[1], Hill G.J.[1] and Bennie S.B.[1]

[1]GNS Science, 1 Fairway Drive, Avalon, Lower Hutt 5010, New Zealand

t.bertrand.nz@gms.cri.nz

Keywords: *Magnetotellurics, Passive-Seismology, Taupo Volcanic Zone, Geothermal Exploration.*

ABSTRACT

Beneath the Taupo Volcanic Zone (TVZ), rocks above the brittle-ductile transition (~7 km depth) have potential to provide a long-term geothermal energy resource for New Zealand. To investigate structures at depths down to ~7 km, detailed passive-seismic and magnetotelluric (MT) data have been collected in the southeastern TVZ. This paper describes the MT data analysis and shows detailed 2-D and initial 3-D inverse resistivity models of profiles that transect the Rotokawa and Ohaaki geothermal systems.

1. INTRODUCTION

The Taupo Volcanic Zone (TVZ) is a rifted arc that is located in the central North Island of New Zealand (Wilson et al., 1995). Within the TVZ, the central rhyolitic part discharges ~4.2 GW of heat through 23 high-temperature geothermal systems (Bibby et al., 1995). Many of these geothermal systems have been explored to a maximum of 3 km depth and provide 14% of New Zealand's electricity demand. To maintain, or to increase this level of geothermal energy, will require production from depths greater than 3 km where temperatures may approach 400°C.

Seismicity suggests that the brittle-ductile transition occurs at a depth of ~6-7 km (Bibby et al., 1995, Bryan et al., 1999) in the TVZ. The meta-sedimentary basement rocks (greywacke) between 3 and 7 km should therefore contain enough fracture permeability to allow convective heat transport. Bibby et al. (1995), and others (Kissling and Weir, 2005; McLellan et al., 2010) suggest that the shallow (<3 km) geothermal fields in the central TVZ represent the upper portion of rising, high-temperature convection plumes that extend down to an underlying magmatic heat source below the brittle-ductile transition. Recently, Bertrand et al., (2012) showed the first-ever geophysical images of these proposed convection plumes.

In 2008, the government of NZ funded an integrated research program (Hotter and Deeper Exploration Science - HADES; Bignall 2010) to guide future deep exploration in the TVZ. This project included components of structural geology, experimental geochemistry, passive-seismology and MT, to investigate links between the deep magmatic heat source and the shallow hydrothermal systems. The MT and passive-seismic measurements were located in the southeastern part of the TVZ and encompass a variety of geological features (eg. the central rift axis, the eastern edge of the Whakamaru collapse caldera, and the eastern rift shoulder; Figures 1 and 2). The goal of these MT measurements was to provide a comprehensive picture of the electrical resistivity structures down to the brittle-ductile transition, in order to identify zones that may be targeted for deep (3 - 7 km depth) geothermal exploration.

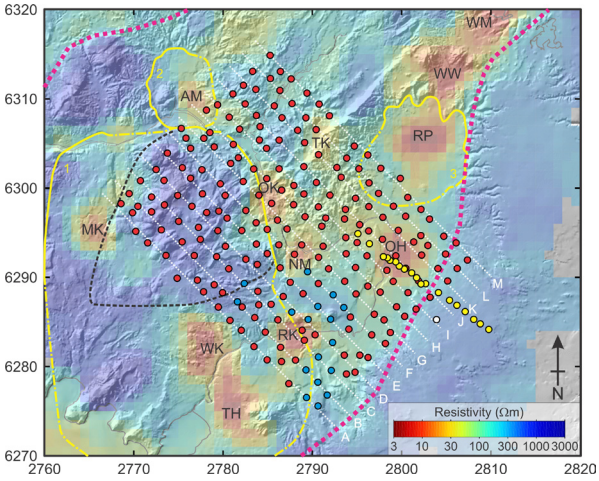

Figure 1: Map of MT data in the southeastern TVZ. Red, blue and yellow circles show MT sites and the white circle is the remote reference. Profiles used in 2-D modeling are shown as white dashed lines (A to M). The background digital elevation model is overlain by the DC apparent resistivity map (Bibby et al., 1995) that correlates low resistivity zones to geothermal systems: TH Tauhara, WK Wairakei, RK Rotokawa, MK Mokai, NM Ngatamariki, OK Orakei-Korako, OH Ohaaki, TK Te Kopia, AM Atiamuri, RP Reporoa, WW Waiotapu-Waikiti, and WM Waimungu. Yellow lines show caldera boundaries (1. Whakamaru, 2. Ohakuri, 3. Reporoa) that intersect the MT array (Wilson and Leonard, 2008). Black dashed line outlines the Maroa volcanic centre, and the pink dashed lines show the approximate boundaries of the TVZ after Wilson et al., 1995.

2. DATA COLLETION AND ANALYSIS

2.1 Passive-Seismic Array

Passive-seismic data were recorded at 40 locations with average site spacing of ~4 km using a rolling array of broadband and short-period seismometers (Figure 2). Both local shallow (<10 km depth) seismicity and earthquakes from the subducted Pacific plate 50-100 km beneath the TVZ were recorded. These data are being used to develop body wave tomography models for Vp, Vp/Vs and Q for the upper crust, imaging depths of 0-15 km. In addition the ambient seismic noise field will be used for surface wave dispersion analysis to generate inter-site Green's functions for periods between 2 and 15 s, for both Love and Rayleigh waves. Figure 2 shows the epicentres of 327 upper crustal (depths <9.5 km) recorded.

2.1 Magnetotelluric Array

Broadband (0.01 - 1000 s) MT data were recorded for 2 nights duration at 204 locations in the southeastern TVZ during the spring months of 2009 and 2010. Measurements were made at ~2 km intervals on a series of profiles that

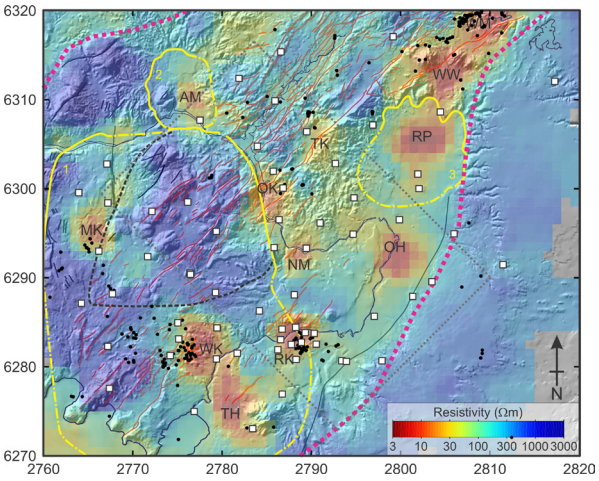

Figure 2: Map of the passive-seismic array in the southeastern TVZ, together with the locations of crustal earthquakes (black dots) recorded in the time period Oct 2009 to Apr 2011. White-squares are seismometer locations and the dashed grey line defines the area of the MT array. Other features are defined in Figure 1.

form a NW-SE rectangular array (25 x 35 km) and extends from the central rift axis to the southeastern rift margin (Figure 1). These profiles are oriented perpendicular to the dominant geological and geoelectric strike directions of the TVZ (i.e. N45°E; Heise et al., 2007). The data collection campaigns were coordinated by GNS Science, and the fieldwork was carried out in collaboration with Auckland University. In total, 9 Phoenix MTU systems were used, including 1 instrument continuously recording at a remote reference site on the Kaingaroa Plateau. Robust processing of the measured time-series data using a remote reference to reduce cultural EM noise (Gamble et al., 1979) resulted in high-quality MT soundings at most sites occupied. In March 2012, GNS Science collected an additional 17 MT sites to fill-in a gap in the existing array (blue circles in Figure 1). MT data were also collected by GNS Science in 2008 for a detailed survey of the Ohaaki geothermal system (yellow circles in Figure 1).

Prior to inversion modeling, the dimensionality of MT data must be assessed to determine if a 1-D, 2-D or 3-D approach is required. The MT phase tensor (Caldwell et al., 2004) provides an effective tool to assess dimensionality that does not make any *a priori* assumptions regarding the regional resistivity structure. In addition, the phase tensor is not significantly affected by galvanic (static-shift) effects (Caldwell et al., 2004) that bias the apparent resistivity data.

Graphically, the phase tensor can be represented by an ellipse that is completely characterized by one direction α, and three coordinate invariants, Φ_{max}, Φ_{min}, and β. For 2-D resistivity structure, the skew-angle $\beta = 0$ and one principal axis of the ellipse (Φ_{max}, Φ_{min}) aligns with the geoelectric strike direction (α or α +90°). For general 3-D structure, β measures deviation from the 2-D case and one principal axis aligns to α - β, defining the direction of greatest inductive response, the closest equivalent to a geoelectric strike (Caldwell et al., 2004). Plotting the α - β values for all periods measured at all sites in the present survey confirms that the overall geoelectric strike direction for these MT data is collinear to the major structural features in the TVZ (i.e. ~N45°E; Figure 3).

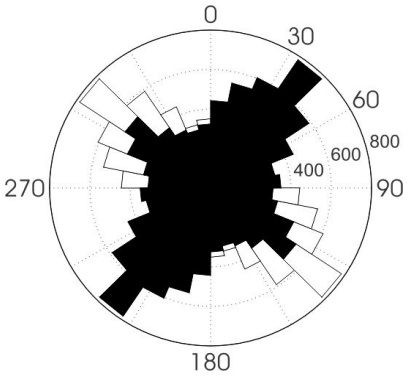

Figure 3: Rose diagram of the phase tensor quantity alpha-beta that is the best approximation of a 2-D geoelectric strike.

Phase tensor ellipses can also be used as an indicator of MT data quality, since spatially coherent patterns should be observable between groups of neighboring sites. Phase tensor ellipses are plotted in Figure 4 and show consistent patterns throughout the entire survey area and period range measured. For example, at periods between 1 and 100 s, the phase tensors rotate 90° across the southeastern boundary of the TVZ (Wilson et al., 1995), and along the scarp of the Paeroa Fault. These rotations indicate along-strike boundaries between zones of low and high resistivity. The overall 2-D nature of the resistivity structure in this region is shown by the alignment at many sites of one phase tensor principal axis to ~N45°E. However, evidence of 3-D structure within the array is also revealed by the arcuate pattern in ellipses (at periods 1 - 10 s) that follow the eastern boundary of the Whakamaru collapse caldera and the Maroa volcanic centre.

In addition to the phase tensor, induction vectors (that are calculated from ratios of the vertical to horizontal magnetic fields) provide independent constraint on MT data dimensionality (Parkinson, 1962). Induction vectors are sensitive to lateral resistivity variations and for 2-D structure should point perpendicular to the geoelectric strike. At periods less than 30 s, induction vectors at sites measured on the Kaingaroa Plateau point northwest (Figure 5) in response to the nearly linear southeast margin of the TVZ. However, at periods greater than 100 s, the induction vectors all rotate to point northeast, indicating a regional-scale 3-D induction effect. These long-period data may be responding to a region of high conductance associated with deep seawater and thick sedimentary basins northeast of the North Island, a common phenomena known as the coast effect (Lilley, 2007).

Close inspection of the induction vectors at periods less than ~10 s (Figure 5) shows that a flip in direction occurs at sites collected on either side of high-voltage power transmission lines that occur within the MT array (Figure 5). This pattern is visible at all sites located within approximately 5 km of a power-line, and indicates that electromagnetic noise in the vertical magnetic fields data is masking the natural MT signals. However, the phase tensor plots (Figure 4) do not show any correlation with the power-lines at these same periods, indicating that this noise phenomenon is restricted to the vertical magnetic fields, or that the remote reference processing has removed any effects from the impedance data. Inversion modeling presented below does not include the induction vector data.

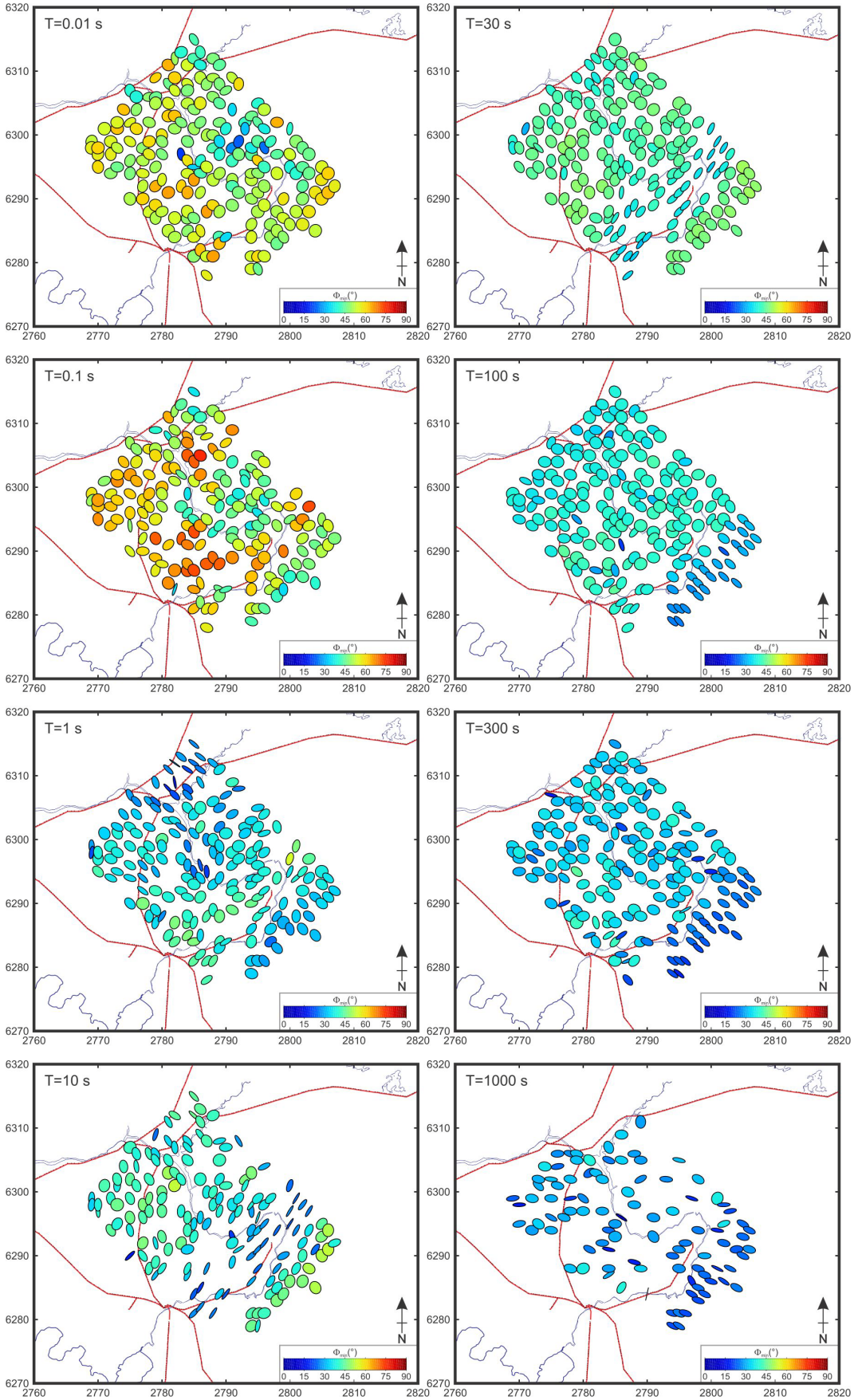

Figure 4: Phase tensor ellipses showing the minimum phase invariant at different periods (T) superimposed on a map of high-voltage power-lines (red) that intersect the MT survey area.

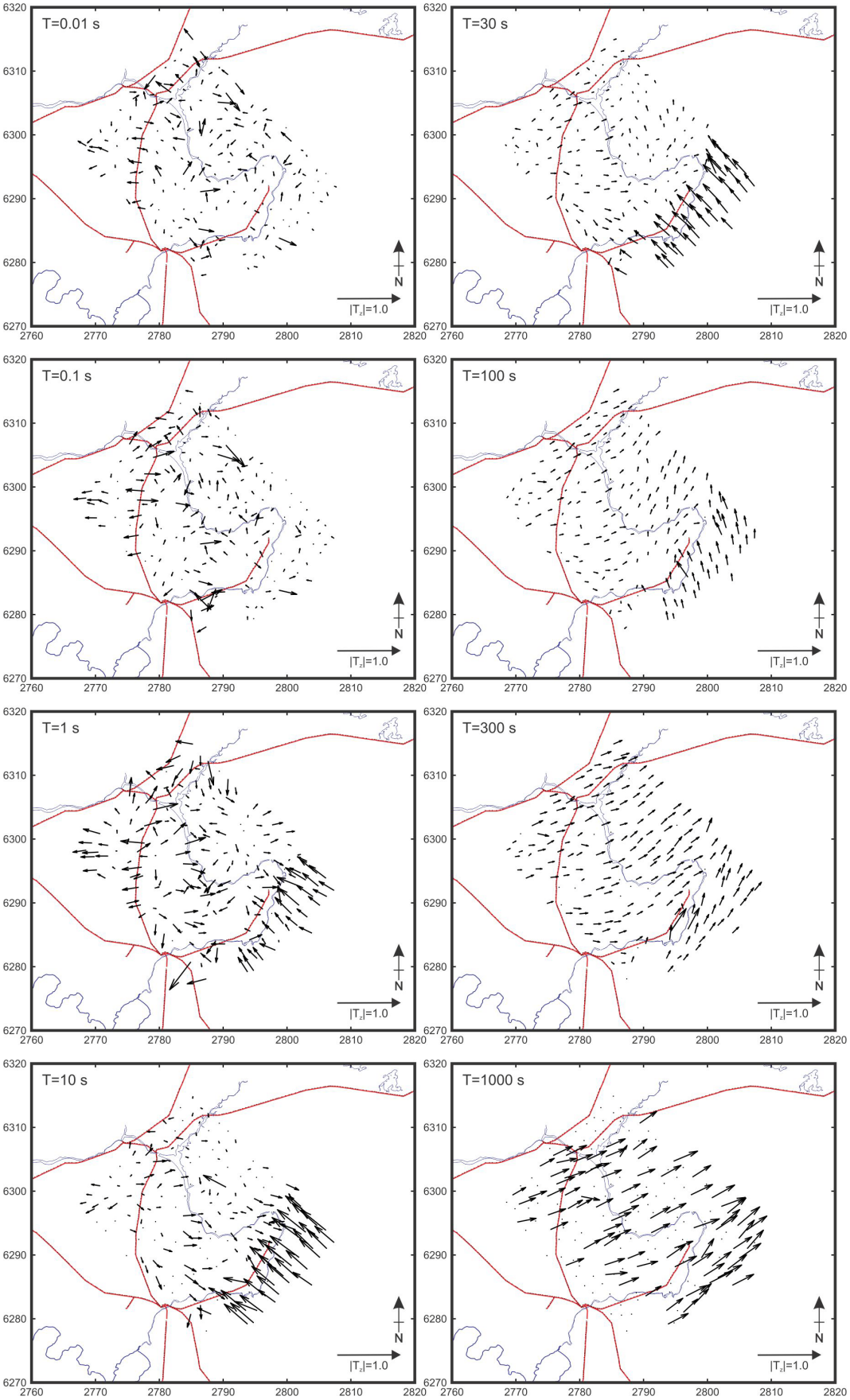

Figure 5: Induction vectors plotted using the Parkinson convention (Parkinson, 1962) at different periods (T) superimposed on a map of high-voltage power-lines (red) that intersect the MT survey area.

3. INVERSION MODELING

3.1 2-D Resistivity Models

Smooth resistivity models of the impedance data were generated for each profile in the array using the 2-D inversion algorithm of Rodi and Mackie (2001). Data points showing high-levels of noise were excluded, and all models achieved root mean square (r.m.s.) misfits between 1.2 and 1.5. Error floors were set to 10% for the apparent resistivity, and 5% for the phase. Setting a larger error floor for the apparent resistivity mitigates the effects of static shifts that do not affect the phase data (Li et al., 2003). The overall smoothing parameter (τ = 1) for the final models was determined by generating an L-curve for each profile (Hansen et al., 1992). Final 2-D models of profiles D and J that intersect the Rotokawa and Ohaaki geothermal systems, respectively, and include the 2012 MT data (blue circles in Figure 1) and the 2008 Ohaaki MT data (yellow circles in Figure 1) are shown in Figure 6.

3.2 Interpretation

In Figure 6 (and also in Figure 3 of Bertrand et al., 2012) the 2-D inversion models show a horizontal band of low-resistivity (10 - 30 Ωm) at depths ranging from the surface down to ~3 km. In places, this low-resistivity layer is overlain by more resistive material >300 Ωm. This shallow resistivity structure confirms similar observations in previous surveys (Ogawa et al., 1999; Heise et al., 2010) and is interpreted as young (< ~700 ka) resistive volcanics overlying older (> ~700 ka) materials that have undergone a diagenetic ageing process that generates conductive clays and zeolites within the mature volcanics (Stanley et al, 1990; Bibby et al., 2005). In general, high resistivity (~1000 Ωm) is imaged from depths of ~3 km down to ~7-8 km, where the resistivity decreases to 10-30 Ωm. Evidence from seismicity suggests that the brittle-ductile transition occurs at ~7 km depth (Bibby et al., 1995), and therefore the deep low resistivities in the MT model are inferred to be caused by a broad layer containing a small amount (~4%) of partial melt (Heise et al., 2007; 2010).

In addition to this background resistivity structure, models D and J reveal zones of low resistivity that connect the deeper magmatic system(s) to near-surface hydrothermal features. Specifically, at Rotokawa field, a vertical pipe-like low-resistivity feature extends downwards from the near surface geothermal system. In contrast, the region directly beneath the Ohaaki geothermal field is resistive, although the area of near-surface low resistivity is connected to a deeper conductive zone that is offset to the northwest.

3.3 3-D Resistivity Models

If the subsurface resistivity structure beneath the MT measurement array were exactly 2-D, then the 2-D resistivity models in Figure 6, that are separated along-strike, should be identical. Clearly, this is not the case, although there is a degree of similarity (an expected result given the underlying 2-D nature of the TVZ). In order to validate the main features in the 2-D models, initial 3-D models of subsets of the MT data were generated.

The 3-D MT inversion algorithm WSINV3DMT (Siripunvaraporn et al. 2005) was used to invert the impedance tensor data collected on profiles B, C, and D through the Rotokawa geothermal system, and for profiles I, J and K through the Ohaaki geothermal system. For each model, 18 periods were inverted, using 4 periods per decade between 0.01 and 1000 s. Error floors were assigned to 20% for the diagonal and 10% for the off-diagonal impedance elements. The model mesh comprised 500 m cell widths between the stations, resulting in x, y, and z dimensions of 46, 98 and 44, respectively. Models ran to convergence using ~12-15 Gb of RAM, and resulted in r.m.s. misfits of 1.1 for both the Rotokawa and Ohaaki models shown in Figure 7. Note that this inversion algorithm does not include static shift or topographic variations, however the model resistivities at 250 m depth agree well with the DC apparent resistivity values (Bibby et al., 1995) suggesting that static and topographic effects are not significant for these data.

An important result is that key features in the 2-D models (Figure 6) are also present in these 3-D models (Figure 7). Specifically, the vertical low-resistivity zone beneath Rotokawa, and the NW dipping zone of low-resistivity beneath Ohaaki are present in both the 2-D and 3-D models.

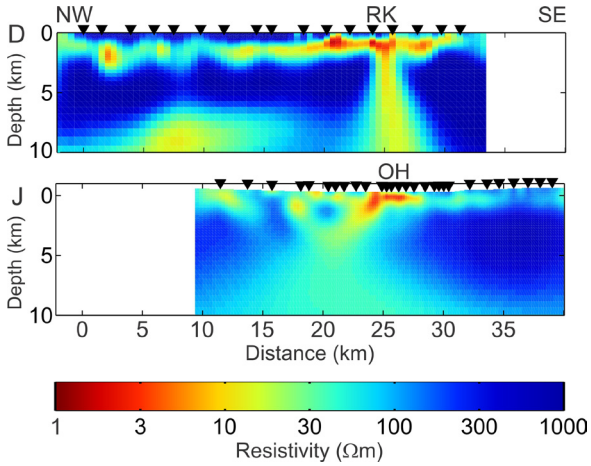

Figure 6: 2-D resistivity models of profile D (including 2012 MT data) through the Rotokawa (RK) geothermal system, and profile J (including 2008 MT data) through the Ohaaki (OH) geothermal system.

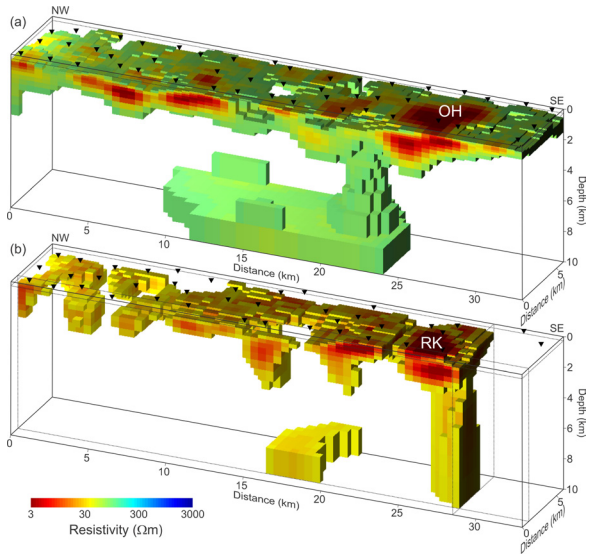

Figure 7: 3-D models of the full MT impedance tensor data for (a) profiles I, J and K through Ohaaki (OH) and (b) profiles B, C and D through Rotokawa (RK), as shown in Figure 1. A resistivity cut-off is used to permit a 3-D view of the vertical (RK) and offset to the north–west (OH) low-resistivity plumes that connect to the surface geothermal fields (Bertrand et al., 2012).

4. CONCLUSIONS

MT and passive-seismic measurements were made to investigate structures in brittle rocks at depths of 3-7 km beneath the southeastern TVZ. Analysis of the MT data show geophysical evidence of connections between the near-surface hydrothermal systems and the underlying magmatic system(s) at depths below ~7-8 km (Bertrand et al., 2012).

ACKNOWLEDGEMENTS

Cooperation from landowners in the survey area is greatly appreciated. We thank Weerachai Siripunvaraporn for use of his 3-D inversion program, WSINV3DMT. This research was funded by the New Zealand Ministry of Science and Innovation.

REFERENCES

Bertrand, E.A., Caldwell, T.G., Hill, G.J., Wallin, E.L., Bennie, S.L., Cozens, N., Onacha, S.A., Ryan, G.A., Walter, C., Zaino, A., and P. Wameyo, Magnetotelluric imaging of upper-crustal convection plumes beneath the Taupo Volcanic Zone, New Zealand: *Geophysical research letters, 39(2):* L02304, 2012.

Bibby, H.M., Risk, G.F., T.G. Caldwell and S.L. Bennie, Misinterpretation of Electrical Resistivity Data in Geothermal Prospecting: a Case Study from the Taupo Volcanic Zone: *Proeedings World Geothermal Congress 2005*, Anatalya, Turkey, 2005.

Bibby, H.M., T.G. Caldwell, F.J. Davey and T.H. Webb, Geophysical evidence on the structure of the Taupo Volcanic Zone and its hydrothermal circulation: *Journal of Volcanology and Geothermal Research*, 68, 29-58, 1995.

Bignall, G., Hotter and deeper: New Zealand's research programme to harness its deep geothermal resources: *Proeedings World Geothermal Congress 2010*, Bali, Indonesia, 2010.

Bryan, C. J., S. Sherburn, H. M. Bibby, S. C. Bannister, and A. W. Hurst, Shallow seismicity of the central Taupo Volcanic Zone, New Zealand: Its distribution and nature: *New Zealand Journal of Geology and Geophysics*, 42, 533-542, 1999.

Caldwell, T.G., H.M. Bibby and C. Brown, The magnetotelluric phase tensor: *Geophysical Journal International*, 158, 457-469, 2004.

Gamble, T.D., W.M. Goubeau and J. Clarke, Magnetotellurics with a remote reference: *Geophysics*, 44, 53-68, 1979.

Hansen, P.C., Analysis of discrete ill-posed problems by means of the L-curve: *Society for Industrial and Applied Mathematics*, 34, 561-580, 1992.

Heise, W., Caldwell, T.G., Bibby, H.M. and S.L. Bennie, Three-dimensional electrical resistivity image of magma beneath an active continental rift, Taupo Volcanic Zone, New Zealand: *Geophysical Research Letters*, 37, L10301, 2010.

Heise, W., H.M. Bibby, T.G. Caldwell, S.C. Bannister, Y. Ogawa, S. Takakura and T. Uchida, Melt distribution beneath a young continental rift: The Taupo volcanic zone, New Zealand: *Geophysical Research Letters*, 34, L14313, 2007.

Kissling, W. M., and G. J. Weir, The spatial distribution of the geothermal fields in the Taupo volcanic zone, New Zealand: *Journal of Volcanology and Geothermal Research*, 145, 136-150, 2005.

Li, S., M.J. Unsworth, J.R. Booker, W. Wei, H. Tan and A.G. Jones, Partial melt and or aqueous fluid in the mid-crust of southern Tibet? Constraints from INDEPTH Magnetotelluric data: *Geophysical Journal International*: 153, 289-340, 2003.

Lilley, T., Coast effect of induced currents: *in* Gubbins, D. and E. Herrero-Bervera, eds., Encyclopedia of Geomagnetism and Paleomagnetism: *Encyclopedia of Earth Sciences Series*, Springer, 61-65, 2007.

McLellan, J. G., Oliver, N. H. S., Hobbs, B. E. and J. V. Rowland, Modelling fluid convection stability in continental faulted rifts with applications to the Taupo volcanic zone, New Zealand: *Journal of Volcanology and Geothermal Research*, 190, 109-122, 2010.

Ogawa, Y., Bibby, H. M., Caldwell, T.G., Takakura, S., Uchida, T., Matsushima, N., Bennie, S.L., Tosha, T. and Y. Nishi, Wide-band magnetotelluric measurements across the Taupo Volcanic Zone, New Zealand - preliminary results: *Geophysical Research Letters*, 26, 3673-3676, 1999.

Parkinson, W.D., The influence of continents and oceans on geomagnetic variations: *The Geophysical Journal of the Royal Astronomical Society*, 6, 411-449, 1962.

Rodi, W. and R.L. Mackie, Nonlinear conjugate gradients algorithm for 2-D Magnetotelluric inversion: *Geophysics*, 66, 174-187, 2001.

Siripunvaraporn, W., G. Egbert, Y. Lenbury and M. Uyeshima, Three-dimensional Magnetotelluric inversion: data-space method: *Physics of the Earth and Planetary Interiors*, 150, 3-14, 2005.

Stanley, W.D., W.D. Mooney and G.S. Fuis, Deep crustal structure of the Cascade range and surrounding regions from seismic refraction and magnetotelluric data: *Journal of Geophysical Research*, 95, 19419-19438, 1990.

Wilson, C.J.N. and G.S. Leonard, Slumbering giants: i*n* Graham, I.J. ed., A continent on the move: New Zealand geoscience into the 21st centrury. Geological Society of New Zealand in association with GNS Science, Wellington: *Geological Society of New Zealand miscellaneous publication 124*, 166-169, 2008.

Wilson, C.J.N., B.F. Houghton, M.O. McWilliams, M.A. Lanphere, S.D. Weaver and R.M. Briggs, Volcanic and structural evolution of Taupo Volcanic Zone, New Zealand: a review: *Journal of Volcanology and Geothermal Research*, 68, 1-28, 1995.